Supporting Information

Rectification of charges on r–TiO_2 via Pd–cocatalysts and schottky junctions to produce H_2 for the green energy system†

Ejaz Hussain [a]*, Muhammad Jalil[a], Mehreen Qurban[a], Muhammad Zeeshan Abid[a], Muhammad Asif Khan[b], Minhas Nazir[a], Khezina Rafiq[a]*

[a]Institute of Chemistry, Inorganic Materials Laboratory 52S, The Islamia University of Bahawalpur-63100, Pakistan.

[b]Department of Food Science and Technology, Faculty of Agriculture and Environment, The Islamia University of Bahawalpur-63100, Pakistan.

Corresponding authors: ejaz.hussain@iub.edu.pk; khezina.rafiq@iub.edu.pk

Chemicals

In this work, all chemicals used were of high purity. The chemical are as follows (i) Rutile titania powder (r-TiO_2) purchased from Sigma (99.90% CAS#1317-80-2) (ii) Palladium acetate i.e. $Pd(OAc)_2$ Sigma (99.80% CAS#3375-31-3) (iii) Sodium borohydride ($NaBH_4$) reagent Plus Sigma (99% CAS#16940-66-2) (iv) Ethanol (CH_3CH_2OH) Sigma (95.00% CAS#64-17-5) (v) Methanol anhydrous (CH_3OH) Sigma (99.8% CAS#67-56-1) (vi) Distilled water (99.9% was purchase from PIAS Pakistan).

Characterization

The X-ray diffraction (XRD) patterns were obtained using a Bruker D2-phaser equipped with a LYNXEYE XE-T detector (220 V/50 Hz). A Cu Kα radiation source with a wavelength of 1.5418 Å was employed for the XRD analysis. The 40 kV and 40 mA voltages were used for the X-ray generation. 2θ scanning range was of 10° to 80° with a step size of 0.05° and a scan rate of 2°

min^{-1}. Raman spectrum were obtained using the argon-laser equipped Micro Raman Renishaw spectrometer. ATR mode on a Bruker Alpha Platinum instrument with a spectral range of 4000–400 cm^{-1} was utilized to perform the FTIR characterizations. A UV-VIS spectrometer (V-550i RM; JASCO) was used to analyze the optical characteristics of the Pd/r-TiO2 samples. The results of scanning electron microscopy (SEM) at various scales were obtained using a FEI-Nova NanoSEM-450 electron microscope equipped with an EDX accessory. The JEM-2021 plus LaB6 TEM was utilized to acquire TEM images for additional structural characterizations, with the aim of analyzing impurities, structural flaws in semiconductors, and crystal structure. The ESCALAB QXI X-Ray photoelectron spectrometer is utilized for XPS measurements. The oxidation state of the deposited Pd and other elements of catalysts were assessed by X-ray photoelectron spectroscopy (XPS; ESCALAB 240X; Thermo Fisher Scientific) at 24W with monochromatic Al K excitation. With a 274.9 eV bonding energy, the found spectra were calibrated to the C1s core level. AFM analysis was performed with PARKIN instruments, to determine the mechanical characteristics and location of the loaded metals on the photocatalysts surface. Thermo Fisher Axia Chemi SEM was used to obtain the SEM images.

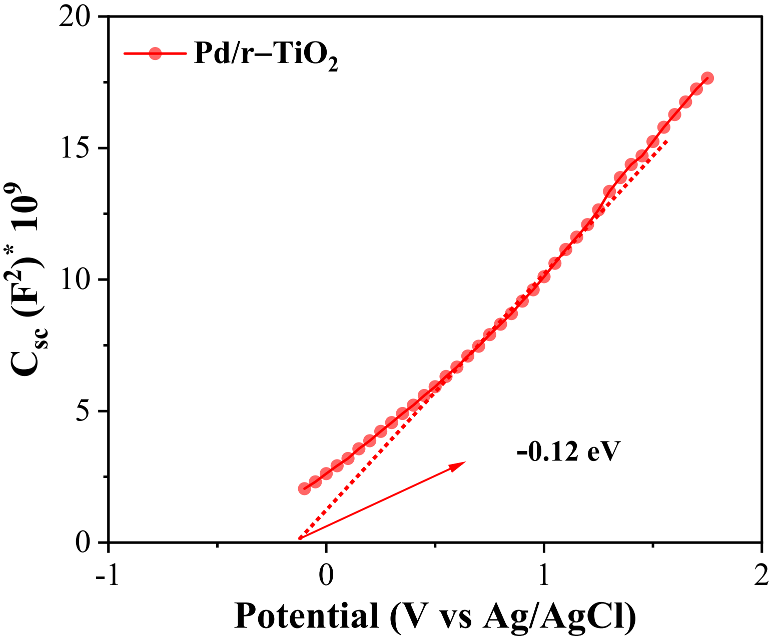

Figure S1: Mott schottky plot for Pd/r-TiO_2 catalysts

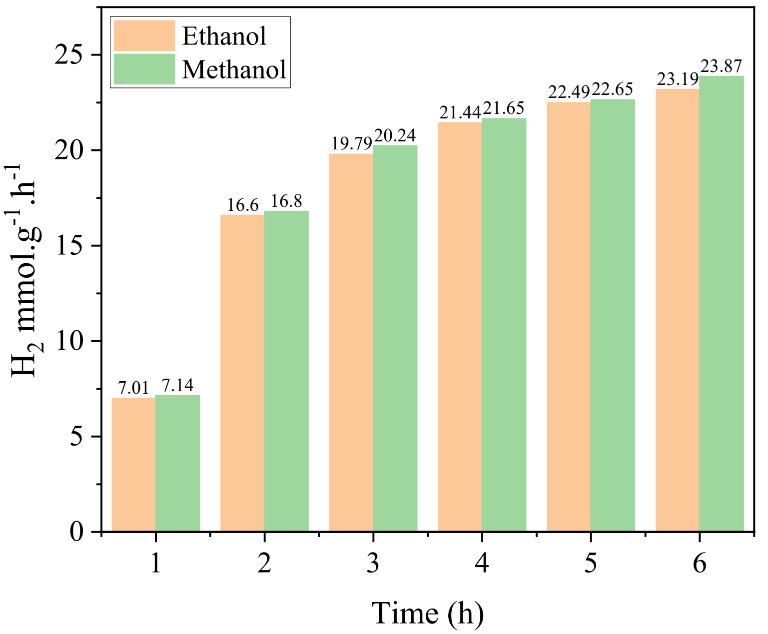

Figure S2: Comparison of H_2 generation activities between ethanol and methanol as sacrificial reagent using Pd/r-TiO_2 catalysts.

Factors affecting the activity of catalysts

pH

pH of the reaction mixture has a considerable impact on photocatalytic hydrogen evolution rate. In this study, hydrogen evolution experiments were carried out at different pH values i.e. pH values from 4 to 12 were taken in the presence of most active Pd/r-TiO_2 catalysts. The maximum hydrogen evolution rate was observed in basic medium i.e. at pH 10 the activity of catalysts was 23.10 $mmolg^{-1}h^{-1}$ as shown in Figure 9(a) & Table S1. At high pH more ^{-}OH ions were present and serve as a hole scavenger to promote the transfer of electrons for reduction reactions at surfaces of catalysts [1]. The results show that the stability of the photocatalysts reduced in both very acidic and basic medium that results decreased in the hydrogen evolution rate [2].

Table S1: Data for the effect of pH.

pH	H_2 ($mmolg^{-1}h^{-1}$)
2	8.45
4	10.45
6	15.67
8	20.65
10	23.10
12	20.65

Temperature

Temperature variation normally do not have a substantial impact on the production of hydrogen thermodynamically [3]. But it was noticed that, temperature have an incredible effect on the adsorption and desorption of hydrogen at the surfaces of photocatalysts. Temperature can alter the overall effectiveness of the catalytic process by altering the adsorption and desorption of hydrogen on the catalyst surfaces, even it is thermodynamically impossible to induce electrons for hydrogen creation [4]. It was observed that as we increased the temperature rate of hydrogen production also increased gradually because with the increase of temperature desorption of hydrogen gas increased from the catalyst surface. High temperatures promote the formation of charges and facilitate the transfer of electrons from the valence band to the conduction band of the semiconductor. Extreme higher temperatures can lead to an increase in the vapor pressure of the reaction mixture, which results decrease in the efficiency of photoreaction [5]. It was observed that, 55°C temperature and pH 10 of the reaction mixture is the ideal one for hydrogen evolution. At these conditions the rate of hydrogen evolution was observed 23.17 $mmolg^{-1}h^{-1}$over most active Pd/r-TiO_2 catalysts see Figure 9(b) & Table S2. These studied demonstrates that the optimization of these factors maximizes the activity of catalysts for hydrogen production.

Table S2: Data for the effect of temperature.

Temperature °C	**H_2 ($mmolg^{-1}h^{-1}$)**
15	15.43
25	16.89
35	18.03
45	21.32
55	23.17
65	21.76

Photocatalysts dose

The rate of hydrogen production was also significantly influenced by the concentration of photocatalyst [6]. In this work, 2.5-12.5 mg dose of Pd/r-TiO_2 photocatalyst was used in 150 mL of Pyrex reactor to evaluate the effect of photocatalyst concentration for the activity of catalyst. It was observed that as the catalyst concentration was increased up to 7.5 mg, the rate of H_2 production increased because more photogenerated charges were available. However, beyond a specific concentration of photocatalyst i.e. 7.5 mg, further additions did not considerably improve the activity of catalyst for hydrogen production [7]. The reduction in activity was attributable to less exposure of the catalyst surfaces to light due the aggregation of catalysts particles. Higher photocatalyst concentration caused particle buildup, which reduced the exposure of light to the active sites of the catalysts [8]. The highest hydrogen production was observed at optimized pH and temperature conditions (pH=10, Temperature =55°C) with optimized photocatalyst dosage of 7.5 mg that was 23.19 $mmolg^{-1}h^{-1}$see Figure 9(c) & Table S3.

Table S3: Data for the effect of catalyst dose.

Catalyst Dose (mg)	**H_2 ($mmolg^{-1}h^{-1}$)**
2.5	12.34
5	20.78
7.5	23.19
10	22.54
12.5	21.34

Intensity of light:

It was observed that increasing light intensity of the light source increases the rate of hydrogen production from water splitting reaction [9]. Figure 9(d) & Table S4 demonstrates that under a light exposure of 550 W/m^2, 23.14 $mmolg^{-1}h^{-1}$of hydrogen was produced using Pd/r-TiO_2 catalysts. This shows that the catalyst was already generating the greatest amount of charges during the photoreaction at this particular light intensity (550 W/m^2), leading to the highest rate of hydrogen production. Beyond this limit, however, the light intensity increase had no discernible effect on the catalyst activity. This means that the catalyst had achieved its saturation point and producing charges for efficient hydrogen generation [10].

Table S4: Data for the effect of light intensity.

Intensity of light (W/m^2)	**H_2 $mmolg^{-1}h^{-1}$**
50	8.54
150	10.67
250	13.58
350	16.98
450	19.67
550	23.14
650	23.46

References

1. Yu, W., et al., *Superb all-pH hydrogen evolution performances powered by ultralow Pt-decorated hierarchical Ni-Mo porous microcolumns.* Advanced Functional Materials, 2023. **33**(4): p. 2210855.
2. Quyyum, U., et al., *Tunable sulphur doping in CuFe 2 O 4 for the efficient removal of arsenic through arsenomolybdate complex adsorption: kinetics, isothermal and mechanistic studies.* Environmental Science: Water Research & Technology, 2023. **9**(4): p. 1147-1160.
3. Yu, J., et al., *Synthesis of carbon-doped KNbO3 photocatalyst with excellent performance for photocatalytic hydrogen production.* Solar Energy Materials and Solar Cells, 2018. **179**: p. 45-56.
4. Xu, H.-Y., et al., *New insights into the photocatalytic mechanism of pristine ZnO nanocrystals: From experiments to DFT calculations.* Applied Surface Science, 2023. **614**: p. 156225.
5. Setiani, P., et al., *Mechanisms and kinetic model of hydrogen production in the hydrothermal treatment of waste aluminum.* Materials for Renewable and Sustainable Energy, 2018. **7**: p. 1-13.
6. Fujita, S.-i., et al., *Photocatalytic hydrogen production from aqueous glycerol solution using NiO/TiO2 catalysts: Effects of preparation and reaction conditions.* Applied Catalysis B: Environmental, 2016. **181**: p. 818-824.
7. Kampouri, S. and K.C. Stylianou, *Dual-functional photocatalysis for simultaneous hydrogen production and oxidation of organic substances.* ACS Catalysis, 2019. **9**(5): p. 4247-4270.
8. Gupta, N. and B. Pal, *Core–shell structure of metal loaded CdS–SiO2 hybrid nanocomposites for complete photomineralization of methyl orange by visible light.* Journal of Molecular Catalysis A: Chemical, 2014. **391**: p. 158-167.
9. Jiang, C., et al., *Photoelectrochemical devices for solar water splitting–materials and challenges.* Chemical Society Reviews, 2017. **46**(15): p. 4645-4660.
10. Rahman, M.Z., K. Davey, and C.B. Mullins, *Tuning the intrinsic properties of carbon nitride for high quantum yield photocatalytic hydrogen production.* Advanced Science, 2018. **5**(10): p. 1800820.